Journal of Zhejiang University-SCIENCE A (Applied Physics & Engineering)
ISSN 1673-565X (Print); ISSN 1862-1775 (Online)
www.zju.edu.cn/jzus; www.springerlink.com
E-mail: jzus@zju.edu.cn

Effect of rich air/fuel ratio and temperature on NO_x desorption of lean NO_x trap*

Lei LIU, Zhi-jun LI†‡, Hong-yang ZHANG, Qing CHANG, Bo-xi SHEN

(*State Key Laboratory of Engines, Tianjin University, Tianjin 300072, China*)

†E-mail: liulei2010@tju.edu.cn

Received June 13, 2013; Revision accepted Sept. 25, 2013; Crosschecked Oct. 16, 2013

Abstract: An experimental and model-based study of the effect of rich air/fuel ratios (AFRs) and temperature on the NO_x slip of a lean NO_x trap (LNT) was conducted in a lean-burn gasoline engine with an LNT after-treatment system. The emissions of the engine test bench and the inlet temperature of the LNT were used as the major inlet boundary conditions of the LNT. The engine periodically operated between a constant lean AFR of 23 with alterable rich AFRs of 10, 11, 12, 13, and 14. A decrease in the rich AFR of the engine strengthened the desorption atmosphere in the LNT, an effect closely related to the number of reductants, and further heightened the NO_x desorption of the LNT, but with a penalty in fuel consumption. To eliminate that penalty, the inlet boundary conditions of the LNT were varied by adjusting the inlet temperature within a range between 200 °C and 400 °C. An increase in inlet temperature heightened the NO_x desorption of the LNT, and a NO_x breakthrough occurred after the inlet temperature exceeded 390 °C. To control NO_x breakthrough, the inlet temperature can be adjusted to offset the strong desorption atmosphere in the LNT commonly created by a rich AFR.

Key words: Lean NO_x trap (LNT), Air/fuel ratio (AFR), Temperature, NO_x adsorption, NO_x desorption
doi:10.1631/jzus.A1300205 **Document code:** A **CLC number:** TK411.5

1 Introduction

With the impending energy crisis and increasing concerns over environmental pollution, energy-savings and emission-reductions have become a worldwide focus. At present, the gasoline engine is the major power source of passenger cars. To meet present energy demands and increasingly stringent engine emission regulations, it is essential to enhance the economy of gasoline engines and reduce their emissions (Guo *et al*., 2006; Martínez-Morales *et al*., 2013). Lean-burn technology is being developed for future engines to achieve a pronounced improvement in fuel economy (Schwarz *et al*., 2006; Baecker *et al*., 2007). The major drawback of lean-burn gasoline engines is the inefficient NO_x conversion of the conventional three way catalyst (TWC) under ultra lean air/fuel ratio (AFR) conditions (König *et al*., 1996). At present, the major methods of NO_x reduction are in-cylinder combustion process improvement (Stokes *et al*., 1994; Iwamoto *et al*., 1997; Lumsden *et al*., 1997) and the highly efficient catalytic technology of after-treatment systems (Hoffmann *et al*., 1997; Brogan *et al*., 1998; Gregory *et al*., 1999).

Catalytic technology of after-treatment systems consists mainly of NO_x direct decomposition (NDD) (Tadao *et al*., 2003), lean NO_x traps (LNTs) (Tabata *et al*., 1995; Gregory *et al*., 1999), and selective catalytic reduction (SCR) (Gieshoff *et al*., 2001). Compared with NDD and SCR, LNTs attract more interest because of their higher NO_x conversion efficiency. LNT technology of lean-burn gasoline engines was

‡ Corresponding author

* Project supported by the National Natural Science Foundation of China (Nos. 50276042, 50776062, and 51276128), the National High Technology R&D Program (863) of China (No. 2008AA06Z322), and the Tianjin Research Program of Application Foundation and Advanced Technology (No. 11JCZDJC23200), China

first proposed by Toyota in the 1990s (Miyoshi *et al*., 1995). A lean-burn gasoline engine with a coupled LNT needs to operate periodically between rich-mode and lean-mode. NO_x emission is adsorbed in an LNT during the lean-mode of the engine. The engine needs to switch to rich-mode when the LNT is close to the saturation point of NO_x storage. After that, large reductants (e.g., H_2, HC, and CO) are generated from the engine and react with the NO_x which is adsorbed in the LNT during the lean-mode of engine. NO_x is then converted to N_2, accompanied by small amounts of NH_3 and N_2O. The reductants are oxidized to H_2O and CO_2 simultaneously. The rich-mode period is shorter than the lean-mode period, so as to lower the fuel consumption of the engine. The storage period of an LNT (the engine in lean-mode) includes only the process of NO_x adsorption, while the regeneration period (the engine in rich mode) includes the processes of NO_x desorption and reduction. Optimization of the LNT in the regeneration period is very challenging because of the short time and multi- process operation. The process of NO_x desorption is more meaningful because it occurs prior to the process of NO_x reduction and determines the number of NO_x which will be reduced by subsequent reductants.

Various simulation models of LNTs have been proposed in the past decade. A NO_x storage model first developed by Olsson *et al.* (2001) was later supplemented with a propylene-based regeneration model (Olsson *et al*., 2002). The major drawback of Olsson's model is that it cannot account for NO adsorption in the presence of O_2. This limitation was removed by Lindholm *et al.* (2008), assuming that NO can be directly adsorbed on $BaCO_3$ and unidentified S_3 sites. Unlike the storage models, the regeneration model proposed by Larson *et al.* (2008) is highly globalized. There are also many regeneration models being proposed based on variable reductants (Koci *et al*., 2009; Digiulio *et al*., 2012).

Although models have been developed from chemical experiments, few such models have been coupled with a real-time engine test bench. In the present study, the process of NO_x purification (NO_x adsorption, desorption, and reduction) was analyzed separately. The NO_x purification of an LNT was based on the actual exhaust of the engine. In addition, the process of switching from the adsorption to desorption periods was investigated thoroughly. The contrasting effects of rich AFRs and temperature on NO_x desorption in the LNT were analyzed in detail so as to find an innovative technology path to achieve better NO_x desorption of the LNT without a penalty in fuel consumption.

2 Experimental setup and methodology

The layout of the lean-burn gasoline engine test bench is shown in Fig. 1. A modified lean-burn gasoline engine CA3GA2 (Tianjin FAW XIALI Automobile Co., Ltd., China) (a port fuel injection (PFI) gasoline engine with three in-line cylinders, 12 valves and a displacement volume of 1 L) was selected. The engine bench tests were carried out at a speed of 2800 r/min with a load of 0.3 MPa. The rich-lean period of the engine was fixed at 7:56. The concentrations of NO_x, O_2, CO, CO_2, and HC in the exhaust were monitored by an exhaust analyzer (model MEXA-7100, Horiba, Japan). The experimental LNT consisted of cylindrical flow-through monolith bricks (110 mm diameter, 200 mm length) containing square channels at a density of 400 channels per square inch (cpsi). The washcost was $Pt/BaO/Al_2O_3$. The model of the LNT was based mainly on Larson *et al.* (2008), but revised by removing reduction reactions. The inlet boundary conditions of the LNT consisted mainly of inlet gases (exhaust gases of the lean-burn gasoline engine) and temperature. The inlet gases of the LNT were measured at a lean AFR of 23 and at rich AFRs of 10, 11, 12, 13 and 14 (Table 1). The inlet temperature of the LNT was adjusted between 200 °C and 400 °C.

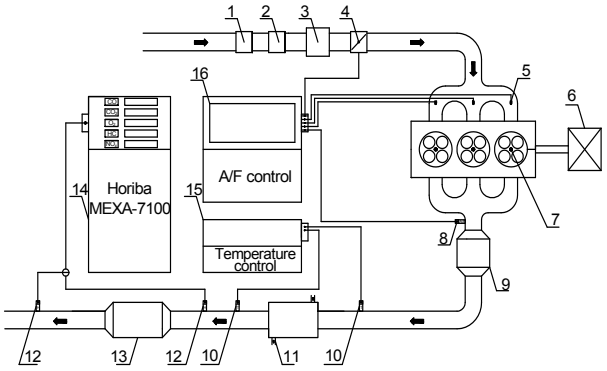

1: air-filter; 2: air-flowmeter; 3: air-chamber; 4: throttle position sensor; 5: fuel injector; 6: dynamometer; 7: spark plug; 8: universal exhaust gas oxygen (UEGO) sensor; 9: three way catalyst (TWC); 10: temperature sensor; 11: cooling water pipe; 12: HORIBA probe; 13: LNT; 14: HORIBA; 15: temperature control; 16: A/F (air/fuel) control

Fig. 1 Layout of the lean-burn gasoline test bench with an LNT

Table 1 Inlet gases of LNT (other inlet gases were regarded as N_2)

AFR of the lean-burn gasoline engine	Inlet flow rate of LNT (g/s)	NO_x ($\times10^{-6}$)	CO ($\times10^{-6}$)	O_2 ($\times10^{-6}$)	CO_2 ($\times10^{-6}$)	HC ($\times10^{-6}$)
23 (lean)	14.4	1199	14.05	68400	106000	58.90
10 (rich)	12.1	22	35664	19945	110727	4232
11 (rich)	12.1	23.6	32922	23672	110363	3911
12 (rich)	12.1	30.4	30180	27400	110000	3590
13 (rich)	12.1	40	27437	31127	109636	3268
14 (rich)	12.1	56	24695	34854	109272	2947

3 Results and discussion

3.1 NO_x slip of LNT

Fig. 2 shows the NO_x slip in the first to the sixth cycles of the LNT at rich AFRs of 10, 11, 12, 13, and 14 with the same fixed inlet temperature of 300 °C. The trends in NO_x adsorption and desorption at those rich AFRs were similar within each cycle, even in the first cycle, which was likely to show irregular trends. However, the trend in NO_x adsorption and desorption in the second to the sixth cycles was different from that in the first cycle. This was mainly because the LNT was in an initialization state with no NO_x adsorbed before the start of the first cycle.

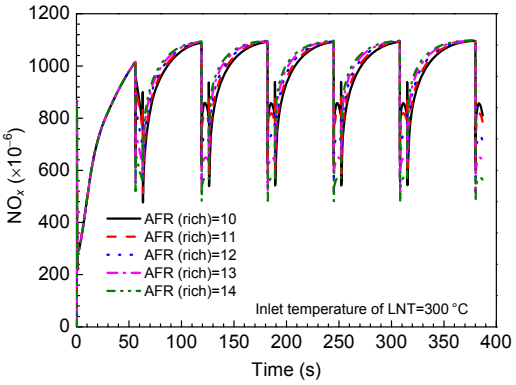

Fig. 2 NO_x slip in the first to the sixth cycles of the LNT

Fig. 3 shows the NO_x slip in the first to the fourth adsorption periods at rich AFRs of 10, 11, 12, 13 and 14. NO_x slip in the first adsorption period was markedly lower than that in the second to the fourth adsorption periods. That was due mainly to the initialization of the LNT mentioned above. The increase in adsorption time heightened the NO_x slip. The main reason is that under the same NO_x flow of the LNT inlet, the increase in adsorption time reduces the number of adsorption sites of the LNT. Also, NO_x slip increased with the increase in rich AFR. The different NO_x slips among different rich AFRs reached a maximum at the beginning of the adsorption period and then decreased to near 0 at the end. That was determined mainly by the NO_x adsorption probability. Specifically, the number of inlet NO_x is assumed to be N, and the total number of adsorption sites in the LNT is assumed to be 100. A completely purified LNT is assumed to be vacant100 (V_{100}) and a completely saturated LNT is assumed to be vacant0 (V_0). Thus, the NO_x adsorption probability is V_x/N, where x is the number of real-time adsorption sites in the LNT. Also, $V_m/N>V_n/N$ can be assumed at the beginning of the adsorption period, where m is the number of NO_x adsorption sites at a rich AFR of 10, and n is the number at a rich AFR of 14. In addition, the number of adsorption sites in the LNT decreased with the increase in adsorption time, which indicates that $V_m/N>V_a/N$ and $V_n/N>V_b/N$, where a is the number of adsorption sites in the LNT after a period of adsorption time at a rich AFR of 10, and b is the number at a rich AFR of 14. Note that a completely saturated LNT is an ideal state which cannot be achieved. V_a and V_b are infinitely close to 0. Thus, $V_a/N\approx V_b/N$ can be assumed. This explains why the difference in NO_x slip among different rich AFRs decreased to near 0 at the end of adsorption period. But to verify the assumption of $V_m/N>V_n/N$, the NO_x slips in the first to the fourth desorption periods at rich AFRs of 10, 11, 12, 13, and 14 are enlarged in Fig. 4.

NO_x slips in the second to the fourth desorption periods were markedly lower and more stable than that in the first desorption period. This was caused mainly by the incomplete desorption of NO_x. Some NO_x absorbed in the previous adsorption period, cannot be desorbed in this desorption period and is

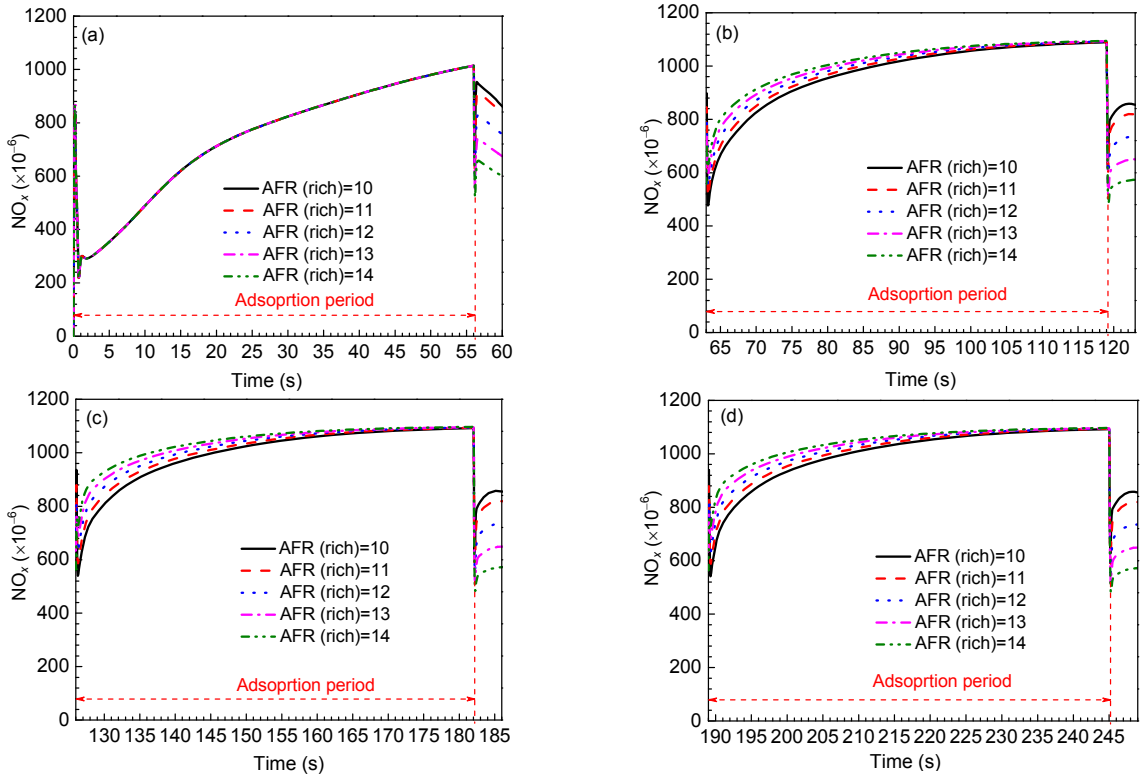

Fig. 3 NO_x slip in the first to the fourth (a)–(d) adsorption periods of the LNT

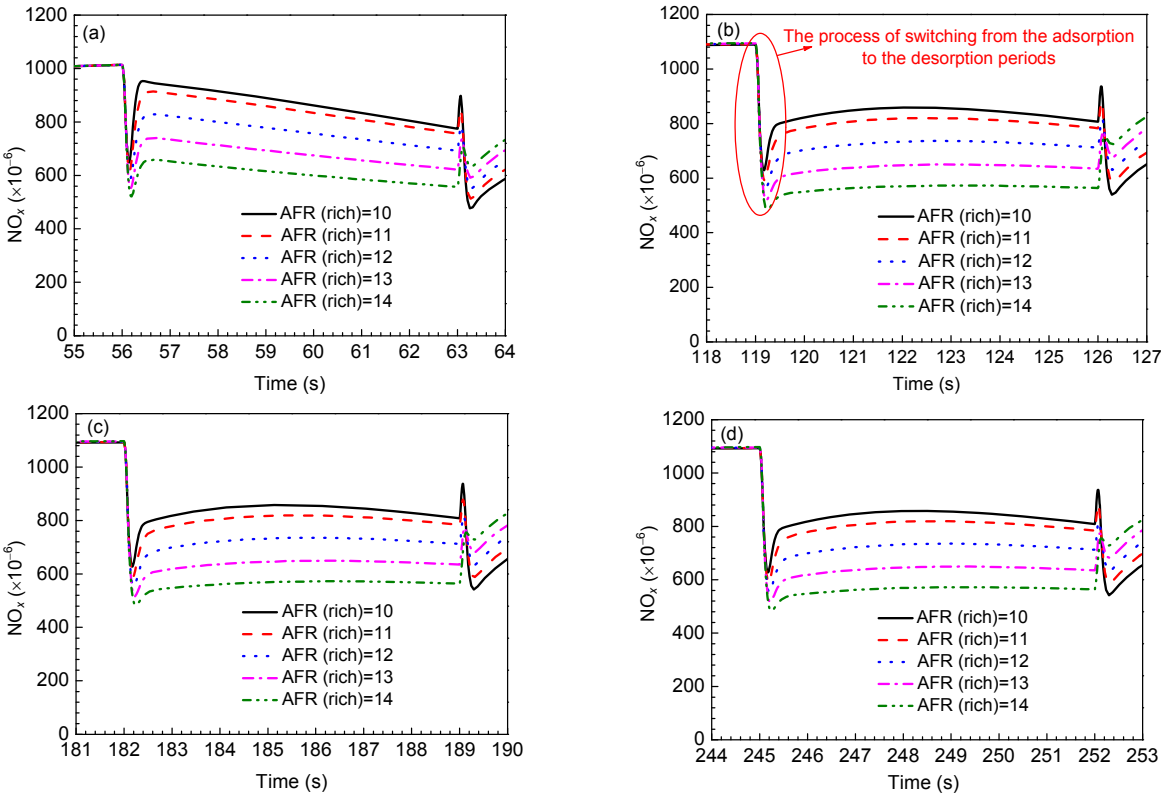

Fig. 4 NO_x slips in the first to the fourth (a)–(d) desorption periods of the LNT

further reduced by reductants. Those adsorption sites that cannot be regenerated are defined as inactive adsorption sites. The number of inactive adsorption sites increased with the increase in the number of cycles and then gradually stabilized. The NO_x slip of the LNT increased with the increase in rich AFR. This indicates that the number of NO_x adsorption sites decreased with the increase in rich AFR at the beginning of the adsorption period, which justifies the above assumption. In addition, the increased level between rich AFRs of 12 and 13 was higher than that between 13 and 14. The increased level between rich AFRs of 11 and 12 was also higher than that between 10 and 11. This implies that for a lean-burn gasoline engine with a rich AFR of 12, whether aiming to achieve higher NO_x conversion efficiency of the LNT or a lower fuel consumption (fuel consumption decreases with the increase in rich AFR), the increased level in NO_x conversion efficiency of the LNT or decreased level in fuel consumption after a rich AFR plus or minus 1 is higher than that after a rich AFR plus or minus more than 1. Moreover, there were fluctuations of NO_x in the process of switching from the adsorption to desorption periods (Fig. 4). This process in the second cycle is enlarged in Fig. 5.

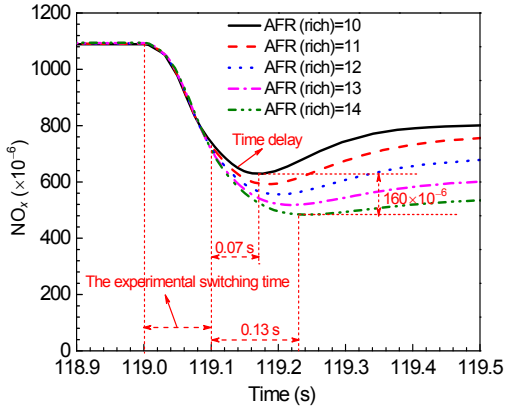

Fig. 5 NO_x slip in the process of switching from the adsorption to the desorption periods in the second cycle of the LNT

Fluctuations in the process of switching from the adsorption to desorption periods occurred at all rich AFRs, but the fluctuation level was very variable. Note that the fluctuation always first decreased to the lowest point and then increased rapidly to a stable level. The moment of minimum NO_x slip signalled the beginning of desorption period. Compared with the theoretical start of desorption period, the actual start point had a time delay. Specifically, the switching time experiment set was 0.1 s (119 s to 119.1 s), while the time delay at rich AFRs of 10 and 14 were 0.07 s and 0.13 s, respectively. The time delay increased with the increase in rich AFR. NO_x slip at the start point of NO_x desorption at a rich AFR of 10 was 160×10^{-6} higher than that at a rich AFR of 14, while the time delay between them was only 0.06 s. This indicates that the time delay in the process of switching from the adsorption to desorption period has a pronounced influence on NO_x slip. The start point of NO_x desorption is influenced by the strength of the desorption atmosphere. The decrease in rich AFR heightened the strength of the desorption atmosphere in the LNT, which is always characterized by the concentration of O_2 and the real-time temperature of the LNT.

3.2 Characterization of the strength of a rich atmosphere: O_2

As one of the major determinants of the strength of the desorption atmosphere in the LNT, O_2 participates mainly in the process of NO_x adsorption and desorption. There are two main paths in the process of NO_x adsorption, the nitrate path and the nitrite path. In the nitrate path, NO is first oxidized to NO_2. Then NO_2 is adsorbed onto a BaO site and forms nitrate. In the nitrite path, NO is directly adsorbed on BaO and forms nitrite, then the nitrite is oxidized to nitrate. Note that, compared with the nitrite path, the nitrate path is more likely to occur in the LNT. This is mainly because, unlike the nitrate path, the nitrite path occurs only at low temperatures. Also, O_2 mainly weakens the desorption atmosphere in the process of NO_x desorption. The strength of the O_2 atmosphere in the adsorption period is determined mainly by the contrast between the NO and NO_2 slips.

Fig. 6 shows details of the NO and NO_2 slips in the second desorption period at rich AFRs of 10, 11, 12, 13, and 14. The decrease in the rich AFR reduced the concentration of O_2. This is indicated by the NO_x slip (NO and NO_2 slips) increasing with the decrease in the rich AFR. In addition, note that the decrease in the rich AFR heightened the NO slip but lowered the NO_2 slip. This indicates there was not enough O_2 to oxidize NO to NO_2 after it weakened the desorption atmosphere.

3.3 Characterization of the strength of a rich atmosphere: temperature

Compared with the desorption atmosphere created by the decrease in the rich AFR of the engine, the desorption atmosphere created by the internal temperature of the LNT was more efficient, and without a penalty in fuel consumption.

Fig. 7 shows the real-time temperature of the LNT at rich AFRs of 10, 11, 12, 13 and 14 with the same fixed inlet temperature of 300 °C. The real-time internal temperature of the LNT rose from 300 °C to between 511 °C and 601 °C. This increase was mainly because of exothermic reactions in the desorption period. The heat generated from exothermic reactions breaks the bonds between adsorption sites and NO_x, which contributes to the large NO_x desorption and is beneficial for the reduction of NO_x to N_2. The decrease in rich AFR raised the real-time internal temperature of the LNT.

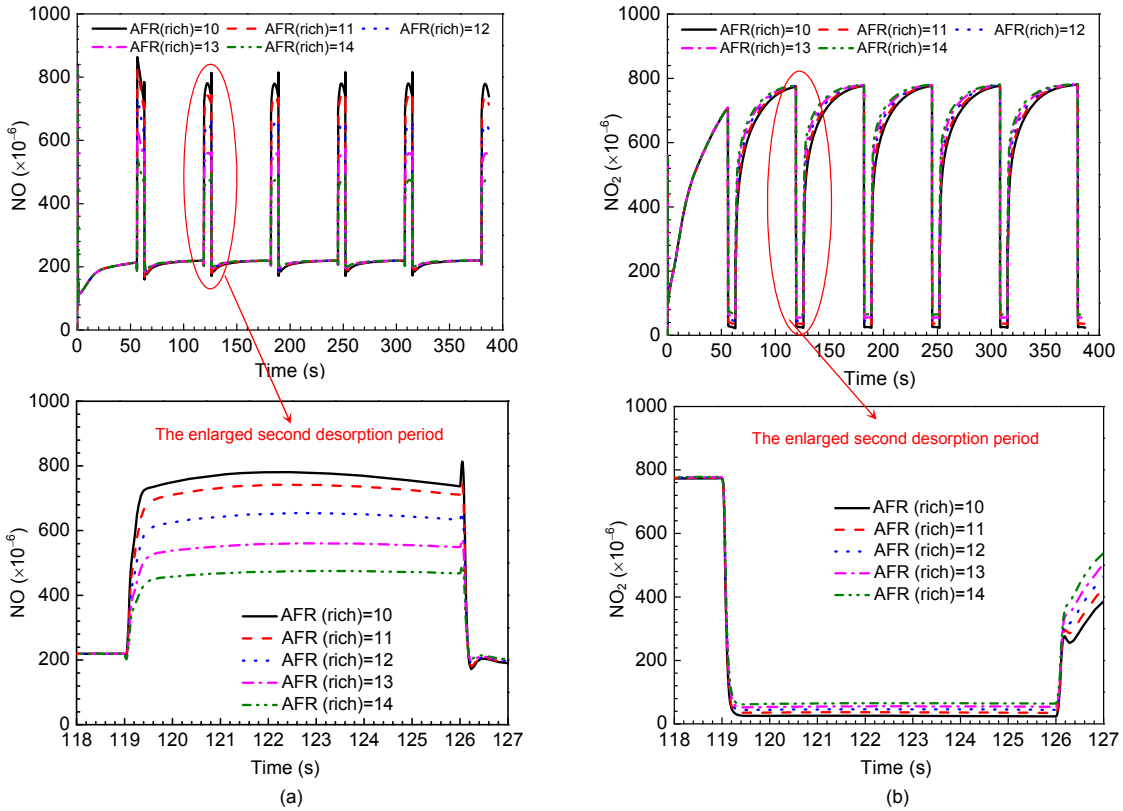

Fig. 6 NO (a) and NO_2 (b) slips in the second desorption period of the LNT

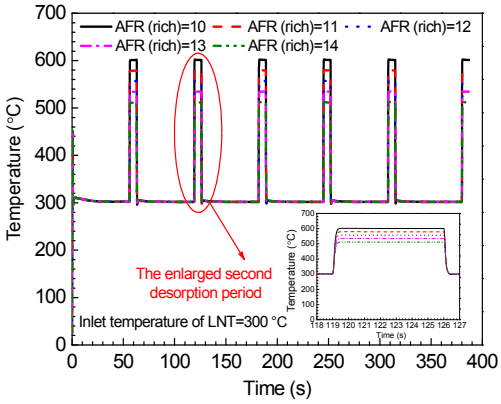

Fig. 7 Real-time internal temperature in the first to the sixth cycles of the LNT

To compare the effects of inlet temperature and rich AFRs on NO_x desorption of the LNT, inlet temperatures of 200 °C and 400 °C were selected (Fig. 8).

Fig. 8 shows the NO_x slip in the first to the sixth cycles of the LNT at rich AFRs of 10, 11, 12, 13, and 14 with an inlet temperature of 300 °C, and at inlet temperatures of 200 °C and 400 °C with a rich AFR of 12. The NO_x slips in the adsorption and desorption periods varied greatly among the inlet temperatures of 200 °C, 300 °C, and 400 °C. At an inlet temperature of 200 °C, the LNT reached the saturation point at the beginning of the adsorption period with little NO_x adsorbed. Likewise, little NO_x was desorbed from the

LNT in desorption period. However, NO_x adsorption and desorption at an inlet temperature of 400 °C had the opposite effect. In the second to the sixth cycle, NO_x adsorption at a rich AFR of 12 with an inlet temperature of 400 °C was also higher than that at an inlet temperature of 300 °C with rich AFRs of 10, 11, 12, 13, and 14. This is attributable to the better NO_x desorption in the first desorption period at a rich AFR of 12 with an inlet temperature of 400 °C. Note that from the enlarged process of NO_x adsorption and desorption, the start point of NO_x desorption at a rich AFR of 12 with an inlet temperature of 400 °C was earlier than in other cases. This implies that the inlet temperature of the LNT has an obvious effect on the start point of the NO_x slip in desorption period, which is similar to the rich AFR effect. In addition, the NO_x slip increased directly to the highest point at a rich AFR of 12 with an inlet temperature of 400 °C, unlike in other cases where it first decreased to the lowest point and then increased rapidly to a stable level. The NO_x breakthrough, such as happened at a rich AFR of 12 with an inlet temperature of 400 °C, is related to temperature and needs to be controlled within a certain range. Less NO_x breakthrough promotes NO_x desorption. A large NO_x breakthrough cannot be reduced by reductants effectively and quickly, and tends to slip out of the LNT directly without being purified.

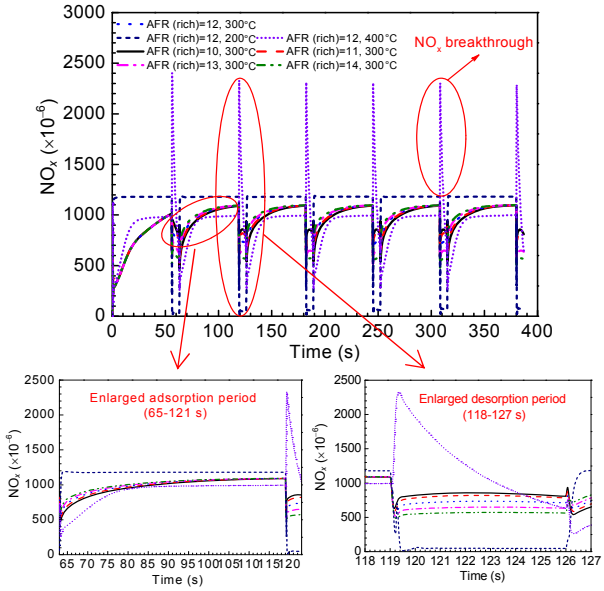

Fig. 8 Effect of rich AFR and inlet temperature on NO_x slip

Fig. 9 shows the effect on NO_x slip of inlet temperatures between 300 °C and 400 °C. The actual start point of NO_x desorption at all inlet temperatures had a time delay. An increase in inlet temperature lowered the time delay. In addition, an increase in inlet temperature increased the NO_x slip. Compared with the start point of NO_x desorption at an inlet temperature of 400 °C, the time delay at an inlet temperature of 300 °C was only 0.15 s, while the difference in NO_x slip was 400×10^{-6}. Note that the maximum difference in NO_x slip between inlet temperatures of 400 °C and 300 °C was 1600×10^{-6} (Fig. 9). This was due mainly to the NO_x breakthrough. The lowest temperature which resulted in NO_x breakthrough was 390 °C.

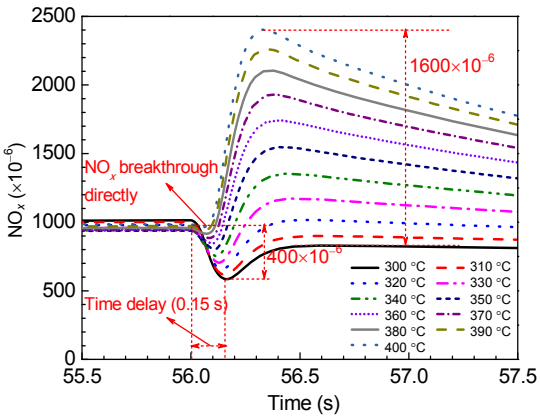

Fig. 9 Effect of inlet temperature on NO_x slip

4 Conclusions

The optimization of NO_x desorption is beneficial for NO_x reduction and adsorption in the next cycle, and may increase the NO_x conversion efficiency of an LNT. An increase in the rich AFR of the engine was beneficial for NO_x adsorption and desorption in the LNT. NO_x adsorption was greatly influenced by NO_x desorption in the previous cycle. Differences in NO_x slip among different rich AFRs gradually decreased to near 0 at the end of the adsorption period, but remained stable throughout the whole desorption period. The strength of the desorption atmosphere created by a rich AFR can be compensated by adjusting the inlet temperature, without a penalty in fuel consumption. Temperature was the major factor affecting NO_x breakthrough.

References

Baecker, H., Kaufmann, A., Tichy, M., 2007. Experimental and simulative investigation on stratification potential of spray-guided GDI combustion systems. *SAE Technical Paper*, 2007-01-1407. [doi:10.4271/2007-01-1407]

Brogan, M.S., Clark, A.D., Brisley, R.J., 1998. Recent progress in NO_x-trap technology. *SAE Technical Paper*, 980933. [doi:10.4271/980933]

Digiulio, C.D., Komvokis, V.G., Amiridis, M.D., 2012. In situ FTIR of the role of surface isocyanates in the reduction of NO_x by CO and C_3H_6 over model $Pt/BaO/Al_2O_3$ and $Rh/BaO/Al_2O_3$ NO_x storage and reduction (NSR) catalysts. *Catalysis Today*, **184**(1):8-19. [doi:10.1016/j.cattod.2011.11.022]

Gieshoff, J., Pfeifer, M., Schäfer-Sindlinger, A., Spurk P.C., Garr, G., Leprince, T., Crocker, M., 2001. Advanced urea SCR catalysts for automotive applications. *SAE Technical Paper*, 2001-01-0514. [doi:10.4271/2001-01-0514]

Gregory, D., Marshall, R.A., Eves, B., Dearth, M., Hepburn, J., Brogan, M., Swallow, D., 1999. Evolution of lean NO_x -trap on PFI and DISI lean burn vehicles. *SAE Technical Paper*, 1999-01-3498. [doi:10.4271/1999-01-3498]

Guo, H., Zhang, Q., Shi, Y., Wang, D.H., Ding, S.Y., Yan, S.S., 2006. Characterization of on-road CO, HC and NO emissions for petrol vehicle fleet in China city. *Journal of Zhejiang University-SCIENCE B*, **7**(7):532-541. [doi:10.1631/jzus.2006.B0532]

Hoffmann, M., Hori, M., Kreuzer, T., Leyrer, J., Lox, E.S., 1997. Lean NO_x catalysis to gasoline fueled European cars. *Journal of Automobile Engineering*, **105**(2):133-135.

Iwamoto, Y., Noma, K., Nakayama, O., Yamauchi, T., Ando, H., 1997. Development of gasoline direct injection engine. *SAE Technical Paper*, 970541. [doi:10.4271/970541]

Koci, P., Plat, F., Stepanek, J., Bartova, S., Marek, M., Kubicek, M., Schmeisser, V., Chatterjee, D., Weibel, M., 2009. Global kinetic model for the regeneration of NO_x storage catalyst with CO, H_2 and C_3H_6 in the presence of CO_2 and H_2O. *Catalyst Today*, **147S**:S257-S264. [doi:10.1016/j.cattod.2009.07.036]

König, A., Richter, T., Jobson, E., Preis, M., Leveroni, E., Krutzsch, B., Noirot, R., Chevrier, M., 1996. Research results on processes and catalyst materials for lean NO_x conversion. *SAE Technical Paper*, 962041. [doi:10.4271/962041]

Larson, R.S., Pihl, J.A., Chakravarthy, V.K., Toops, T.J., Draw, C.S., 2008. Microkinetic modeling of lean NO_x trap chemistry under reducing conditions. *Catalysis Today*, **136**(1-2):104-120. [doi:10.1016/j.cattod.2007.12.117]

Lindholm, A., Currier, N.W., Li, J., Yezerets, A., Olsson, L., 2008. Detailed kinetic modeling of NO_x storage and reduction with hydrogen as the reducing agent and in the presence of CO_2 and H_2O over a Pt/Ba/Al catalyst. *Journal of Catalysis*, **258**(1):273-288. [doi:10.1016/j.jcat.2008.06.022]

Lumsden, G., Eddleston, D., Sykes, R., 1997. Comparing lean burn and EGR. *SAE Technical Paper*, 970505. [doi:10.4271/970505]

Martínez-Morales, J.D., Palacios-Hernández, E.R., Velázquez-Carrillo, G.A., 2013. Modeling and multi-objective optimization of a gasoline engine using neural networks and evolutionary algorithms. *Journal of Zhejiang University-SCIENCE A (Applied Physics & Engineering)*, **14**(9):657-670. [doi:10.1631/jzus.A1300010]

Miyoshi, N., Matsumoto, S., Katoh, K., Tanaka, T., Harada, J., Takahashi, N., Yokota, K., Sugiura, M., Kasahara, K., 1995. Development of new concept three-way catalyst for automotive lean-burn engines. *SAE Technical Paper*, 950809. [doi:10.4271/950809]

Olsson, L., Persson, H., Fridell, E., Skoglundh, M., Andersson, B., 2001. Kinetic study of NO oxidation and NO_x storage on Pt/Al_2O_3 and $Pt/BaO/Al_2O_3$. *Journal of Physical Chemistry B*, **105**(29):6895-6906. [doi:10.1021/jp010324p]

Olsson, L., Fridell, E., Skoglundh, M., Andersson, B., 2002. Mean field modelling of NO_x storage on $Pt/BaO/Al_2O_3$. *Catalysis Today*, **73**(3-4):263-270. [doi:10.1016/S0920-5861(02)00009-3]

Schwarz, C., Schünemann, E., Durst, B., Fischer, J., Witt, A., 2006. Potentials of the spray-guided BMW DI combustion system. *SAE Technical Paper*, 2006-01-1265. [doi:10.4271/2006-01-1265]

Stokes, J., Lake, T.H., Christle, M.J., Denbratt, I., 1994. Improving the NO_x/fuel economy tradeoff for gasoline engine with CCVS combustion system. *SAE Technical Paper*, 940482. [doi:10.4271/940482]

Tabata, M., Yamamoto, T., Fukube, T., 1995. Improving NO_x and fuel economy for mixture injected SI engine with EGR. *SAE Technical Paper*, 950684. [doi:10.4271/950684]

Tadao, N., Juhana, R., Manabu, M., 2003. A new NO_x direct catalytic decomposition on a Rh-based catalyst. *SAE Technical Paper*, 2003-01-3243. [doi:10.4271/2003-01-3243]